Sensors **2008**, *8*, 8262-8274; DOI: 10.3390/s8128262

OPEN ACCESS

sensors

ISSN 1424-8220

www.mdpi.com/journal/sensors

Article

Electrochemical Immunosensor Based on Polythionine/Gold Nanoparticles for the Determination of Aflatoxin B_1

Joseph H.O. Owino, Omotayo A. Arotiba, Nicolette Hendricks, Everlyne A. Songa, Nazeem Jahed, Tesfaye T. Waryo, Rachel F. Ngece, Priscilla G .L. Baker and Emmanuel I. Iwuoha*

SensorLab, Department of Chemistry, University of Western Cape, Private Bag X17, Bellville 7535, Cape Town, South Africa

* Author to whom correspondence should be addressed; E-mail: eiwuoha@uwc.ac.za

Received: 19 September 2008; in revised form: 1 December 2008 / Accepted: 2 December 2008 / Published: 15 December 2008

Abstract: An aflatoxin B_1 (AFB_1) electrochemical immunosensor was developed by the immobilisation of aflatoxin B_1-bovine serum albumin (AFB_1-BSA) conjugate on a polythionine (PTH)/gold nanoparticles (AuNP)-modified glassy carbon electrode (GCE). The surface of the AFB_1-BSA conjugate was covered with horseradish peroxidase (HRP), in order to prevent non-specific binding of the immunosensors with ions in the test solution. The AFB_1 immunosensor exhibited a quasi-reversible electrochemistry as indicated by a cyclic voltammetric (CV) peak separation (ΔE_p) value of 62 mV. The experimental procedure for the detection of AFB_1 involved the setting up of a competition between free AFB_1 and the immobilised AFB_1-BSA conjugate for the binding sites of free anti-aflatoxin B_1 (anti-AFB_1) antibody. The immunosensor's differential pulse voltammetry (DPV) responses (peak currents) decreased as the concentration of free AFB_1 increased within a dynamic linear range (DLR) of 0.6 - 2.4 ng/mL AFB_1 and a limit of detection (LOD) of 0.07 ng/mL AFB_1. This immunosensing procedure eliminates the need for enzyme-labeled secondary antibodies normally used in conventional ELISA–based immunosensors.

Keywords: Immunosensor; Gold nanoparticles; Aflatoxin B_1; Polythionine; Horseradish peroxidise (HRP).

---

1. Introduction

Aflatoxin B_1 (AFB_1) is an example of a group of highly toxic difurancoumarin derivatives that are produced by many strains of *Aspergillus flavus* and *A. parasiticus* which often contaminate a variety of food and animal feed stored under temperate and humid conditions favourable to mould growth [1]. The four major aflatoxins have been designated as B_1, B_2, G_1 and G_2 based on their fluorescence under UV light and their relative chromatographic mobility during thin layer chromatography. AFB_1 has been classified as a group 1 human carcinogen and aflatoxins G_1, G_2 and B_2 belong to a group human carcinogens [2]. These toxins exhibit carcinogenic, teratogenic and mutagenic properties and have now been isolated from a wide variety of agricultural products [3]. AFB_1 can enter the food chain mainly through the ingestion of contaminated human or animal food. The intake of AFB_1 over a long period of time, even in low concentrations, may be very deleterious to health [4]. The Food and Agricultural Organization 2004 report on mycotoxins [5] revealed that as of December 2003, at least 99 countries worldwide had regulations in place for permitted mycotoxin levels in food/or feed, and have set limits for AFB_1 alone or for the sum of aflatoxins B_1, B_2, G_1 and G_2. The maximum permissible level for AFB_1 in food was set at 2 μg/kg (2 ppb).

Many analytical methods have been developed for the determination of aflatoxins. These include thin-layer chromatography (TLC) [6] and high-performance liquid chromatography (HPLC) [7]. Though these techniques have excellent sensitivities they typically require skilled operators, extensive sample pre-treatment and expensive equipment [8]. The goal of more recent studies has been to simplify and expedite the method of detection while attempting to maintain or improve the sensitivity. Among the immunochemical approaches, the enzyme-linked immunosorbent assay (ELISA) method is the most widely applied. Spectrophotomeric ELISAs specific for AFB_1 [9, 10], total aflatoxins [11, 12] and AFM_1 [13, 14] have been developed and their simplicity, adaptability and sensitivity have been demonstrated. In order to achieve higher sensitivity and move to the use of disposable probes, electrochemical immunosensors for aflatoxins based on indirect competitive ELISA format have been proposed [15-17]. These immunosensors require the use of labeled secondary antibodies for detection. To achieve label-free immunosensors, direct electrochemical immunosensors for AFB_1 based on electrochemical impedance spectroscopy [18], optical waveguide lightmode spectroscopy [19] and room temperature ionic liquids [20] have been reported.

The search for a simple and label-free amperometric immunosensor is of considerable interest. Among the various conducting polymers, thionine (phenothiazine) is a redox dye which has been studied extensively due to its potential utility in sensor applications [21, 22]. Its electroactivity lies not only in the heterocyclic nitrogen atoms and nitrogen bridges, but also in its free amine groups [23]. In addition polythionine (PTH) can be easily functionalised due to the abundant amino groups which adsorb metal ions and various organic halogen substances, thus preventing proteins from damage [24].On the other hand, gold nanoparticles (AuNPs) have been extensively used as matrices for the immobilization of macromolecules such as proteins, enzymes and antibodies; as well as chemical labels for biomolecules [25-27]. Modification of electrode surfaces with AuNPs provides a microenvironment similar to what obtains under physiological conditions [28]. In this investigation, an electrochemical immunosensor for the detection of AFB_1 was developed by the drop-coating of AuNPs on PTH-modified glassy carbon electrode (GCE) surface. Subsequently AFB_1-conjugate was

adsorbed on to the gold nanoparticles surface. Details of the preparation, characterization and application of the immunosensor are described.

2. Experimental

2.1 Reagents and materials

Analytical reagent grade chemicals from Sigma-Aldrich were used in all experiments. Phosphate buffer saline (PBS) solution pH 7.2 contained 0.1 M KH_2PO_4, 0.1 M Na_2HPO_4, 2.7 mM KCl and 0.137 M NaCl. Acetate buffer (pH 6.5) was prepared from 0.1 M CH_3COONa, 0.1 M CH_3COOH and 0.1 M KCl. 1 mg/mL Aflatoxin B_1 (AFB_1) solution was prepared by dissolving AFB_1 from *Aspergillus flavus* in methanol followed by dilution in PBS/10% methanol to give a series of standard solutions with a concentration range of 0.1- 3.0 ng/mL. The antibody reagent was an immunoglobin (Ig) fraction of rabbit antiserum AFB_1 (anti-AFB_1) antibody that contained 6.8 mg/mL of total protein (which has reactivity with aflatoxins B_1, G_1 and B_2, but no cross reactivity with B_{2a}, G_2, G_{2a} or M_1) and 0.15 M NaN_3 as preservative. The anti-AFB_1 antibody solution for immunosensing reactions was prepared by diluting the stock 6.8 mg/mL solution to 1:2000 v/v in PBS and stored at -20 ^oC when not in use. Aflatoxin B_1-BSA conjugate (8–12 mol AFB_1 per mol BSA), horseradish peroxidase (HRP; 169 units/mL lyophilised powder; EC.1.11.1.7; M_r 4000), thionine acetate (3,7-diamino-5-phenothiazinium acetate; $C_{12}H_9N_3S.C_2H_4O_2$; M_r 287.34), tetrachloro-auric acid ($HAuCl_4.3H_20$; M_r 393.83), sodium citrate and 30% hydrogen peroxide solution were other reagents used in the studies. Colloidal gold nanoparticles (AuNP) (diameter = 20 nm) were prepared according to the procedure of Yuan et a., 2004 [29] by adding 2 mL of 1% (w/w) sodium citrate to a boiling solution of 50 mL 0.01% (w/w) tetrachloro-auric acid. The AuNP solution was stored in a refrigerator in a dark-colored glass bottle. The production of colloidal AuNP was confirmed by UV-Vis measurement covering 200 – 700 nm at room temperature using distilled water as the reference, which gave a maximum absorption at 520 nm. The particle size of the AuNP was determined with transmission electron microscopy (TEM), in which a sample of the colloidal AuNP was dropped on a carbon-coated copper grid and left to dry for 24 h, after which TEM images were recorded and analysed.

2.2 Instrumentation

All electrochemical experiments were performed with a BAS/50W integrated automated electrochemical workstation (Bioanalytical Systems Lafayette, IN, USA). Cyclic voltammetry and differential pulse voltammetry experiments were performed with Ag/AgCl (3 M NaCl type) and platinum wire as reference and auxiliary electrodes, respectively. A BAS 3-mm diameter GCE in bare or modified form, was used as the working electrode. Transmission electron microscopy studies were carried out with JEOL JEM-1200 EX II electron microscope. UV-Vis experiments were performed with GBC UV/Vis 920 spectrophotometer (GBC Scientific Instruments, Australia).

2.3 Immunosensor preparation

Before use the GCE was polished consecutively with 1.0, 0.3 and 0.05 micron aqueous slurry of alumina micropolish (Buehler, IL, USA), followed by sonication in double-distilled water and ethanol for 5 min and dried in air. 0.1 mM thionine was polymerised on the GCE by cyclic voltammetry (CV) in a 20-voltammetric cycle experiment covering a potential window of -400 to +1200 mV at a scan rate of 50 mV/s and a sensitivity of 0.001 A/V to produce the required PTH. Freshly prepared PTH film was drop-coated with 2 µL of colloidal AuNP and allowed to dry for 24 h. Subsequently the electrode was coated with 5 µL of AFB_1-BSA conjugate (1 µg/mL) and incubated for 1 h at 37 ^oC. The resultant immunosensor was incubated in 1 mg/mL HRP contained in acetate buffer (pH 6.5) for 60 min at 4 ^oC in order to block any remaining active sites of the AuNP layer and avoid non-specific adsorptions. The immunosensor was stored at 4 ^oC when not in use. The schematic illustration of the stepwise immunosensor assembly procedure is shown in Scheme 1.

Scheme 1. Reaction scheme for the preparation of aflatoxin B_1 immunosensor. Step 1: polymerization of thionine. Step 2: formation of AuNP layer. Step 3: loading of AFB_1-BSA conjugate. Step 4: blocking of AFB_1-BSA conjugate layer with HRP.

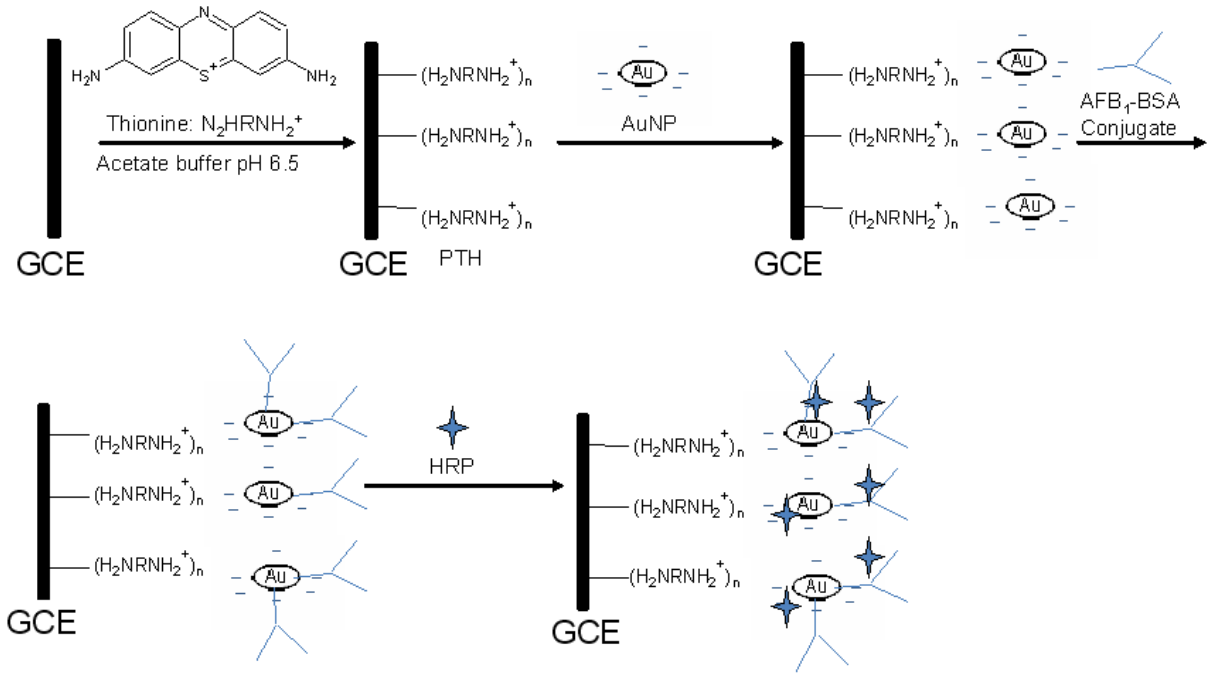

2.4 Procedure for electrochemical immunosensing

Competitive immunosensing was performed in the absence and presence of free AFB_1. Experiment in the absence of free AFB_1 (i.e. 0.0 ng/mL AFB_1) were performed by placing 5 µL of anti-AFB_1 antibody on top of the immunosensor (i.e. GCE|AuNP|PTH|AFB_1-BSA-conjugate HRP) and allowed to react for 15 min. The electrode system was immersed in a 1 mL cell solution containing acetate buffer pH 6.5 and 3.2 µM H_2O_2 and DPV measurement was performed by scanning cathodically from 0 to -480 mV at 10 mV pulse amplitude, 50 ms pulse width and 20 mV/s potential scan rate. For experiments in the presence of free AFB_1 (i.e. 0.6 – 3.0 ng/mL AFB_1), 10 µL of anti-AFB_1 antibody

solution was mixed with 10 μL of 0.6, 1.2, 1.8, 2.4 or 3.0 ng/mL AFB_1 solutions. 5 μL of this mixture was placed on top of the immunosensor and allowed to react for 15 min. This was followed by DPV measurement as described above for 0.0 ng/mL AFB_1.

3. Results and Discussion

3.1 Characterisation of gold nanoparticles

UV-Vis spectrum of the colloidal gold nano-particles prepared by the method of Yuan *et al.* [29] showed a maximum absorption, λ_{max}, at 520 nm (Figure 1). The formation of nano-particles and the particle size (20 nm diameter) were confirmed by the TEM data (Figure 2). These results agreed with what has been reported for colloidal AuNP [29].

Figure 1. UV-Vis spectrum of colloidal gold nanoparticles.

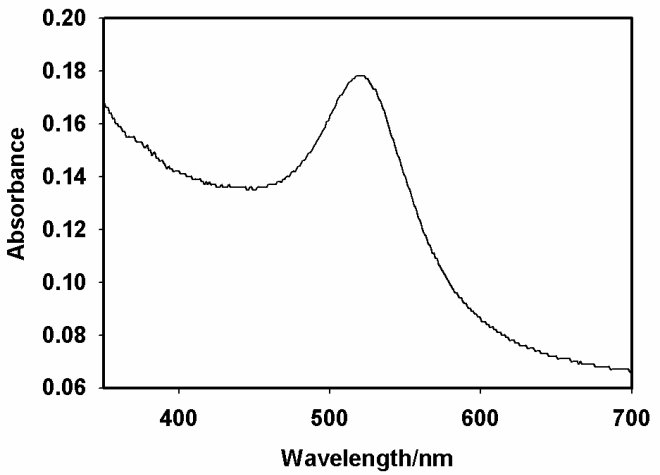

Figure 2. TEM image of colloidal gold nanoparticles.

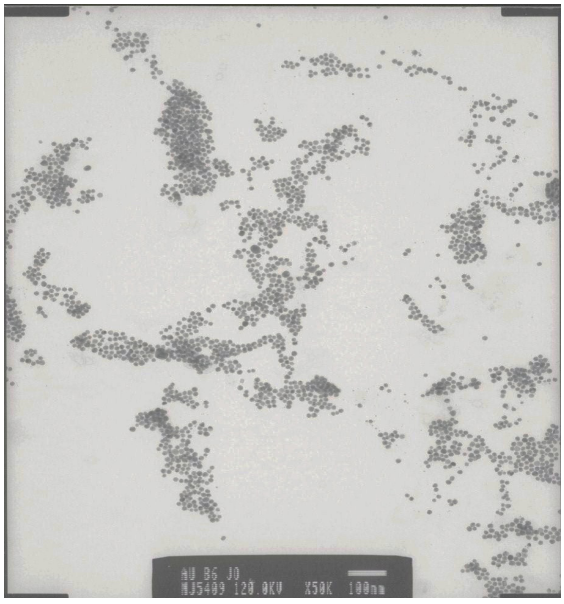

3.2 Electropolymerization of multiporous thionine film

The GCE was first reduced in acetate buffer solution (pH 6.5) containing thionine at -1500 mV to make it negatively charged and interact with positively charged thionine in the mildly acidic conditions. Subsequently cyclic voltammetry was performed at a bias voltage of -400 to +1200 mV at a scan rate of 50 mV/s. When the applied potential exceeded +1100 mV, the electropolymerization reaction proceeded and formed cationic radical species on the GCE [30]. This process resulted in a multiporous structure which facilitated the assembly of AuNP. The oxidation potential in the first step was the most important factor for electropolymerization of thionine and should not be less than +1100 mV. Two reasons suffice for this. Firstly in order to achieve the formation of polythionine (PTH) film, the electrode potential must be larger than the potential at which the oxidations of $–NH_2$ groups of thionine molecule occurs, and secondly the modified cation must be necessarily associated with the surface activation of GCE. During thionine electropolymerization, a pair of quasi reversible redox peaks with a cathodic peak potential (E_{pc}) of -250 mV and an anodic peak potential E_{pa} of -100 mV, increased gradually and tended to become stable with increasing number of polymerization cycles (Figure 3a). On removal of the electrode from the dye-containing solution, a golden film was seen on the electrode surface. The CV of the GCE|PTH in acetate buffer (pH 6.5) (Figure 3b) confirmed the presence of surface-bound electroactive material. Figure 4 shows the scan rate dependence of the electrochemistry of GCE|PTH and GCE|PTH|AuNP|AFB_1-BSA-conjugate electrodes in acetate buffer pH 6.5. The peak currents varied linearly with scan rate as is characteristic of the electrochemistry of a surface-bound thin film of electroactive material [31]. It is thus suggested that nearly all the reduced polythionine ($PTH_{(red)}$) was converted to the oxidized polythionine ($PTH_{(ox)}$) on the forward scan and vice versa.

Figure 3. Cyclic voltammograms (a) for the synthesis of PTH from 0.1 mM thionine in acetate buffer (pH 6.5); and (b) of GCE|PTH in acetate buffer (pH 6.5). (Scan rate: 50 mV/s)

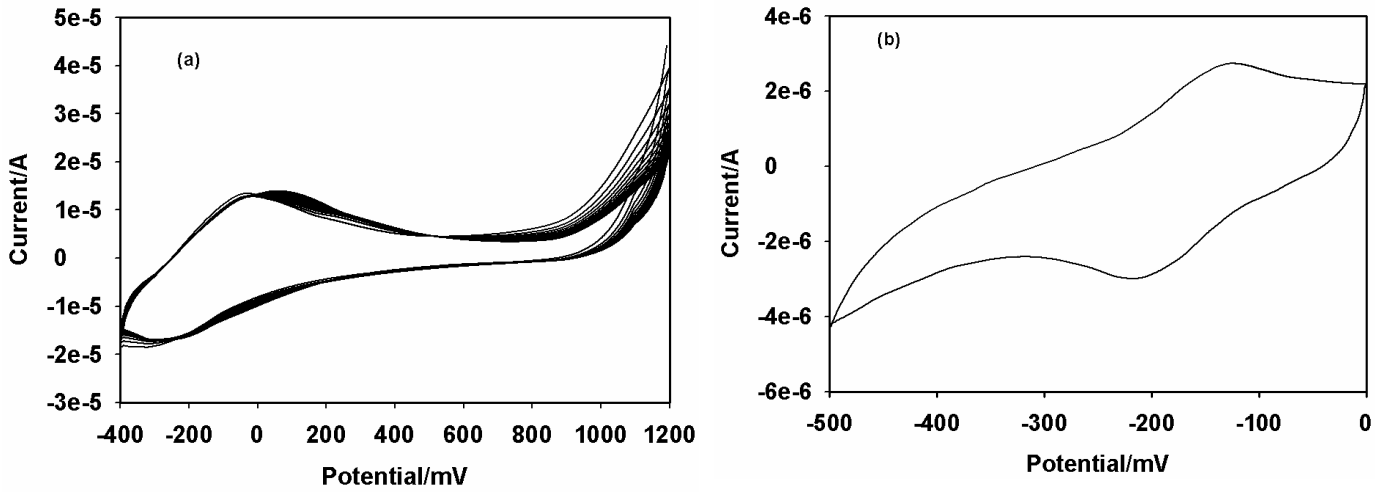

Figure 4. CV's of **(a)** PTH|GCE and **(b)** GCE|PTH|AuNP|AFB_1-BSA-conjugate in acetate buffer (pH 6.5) at 5, 10, 20, 30 and 50 mV/s (starting from the inner CV).

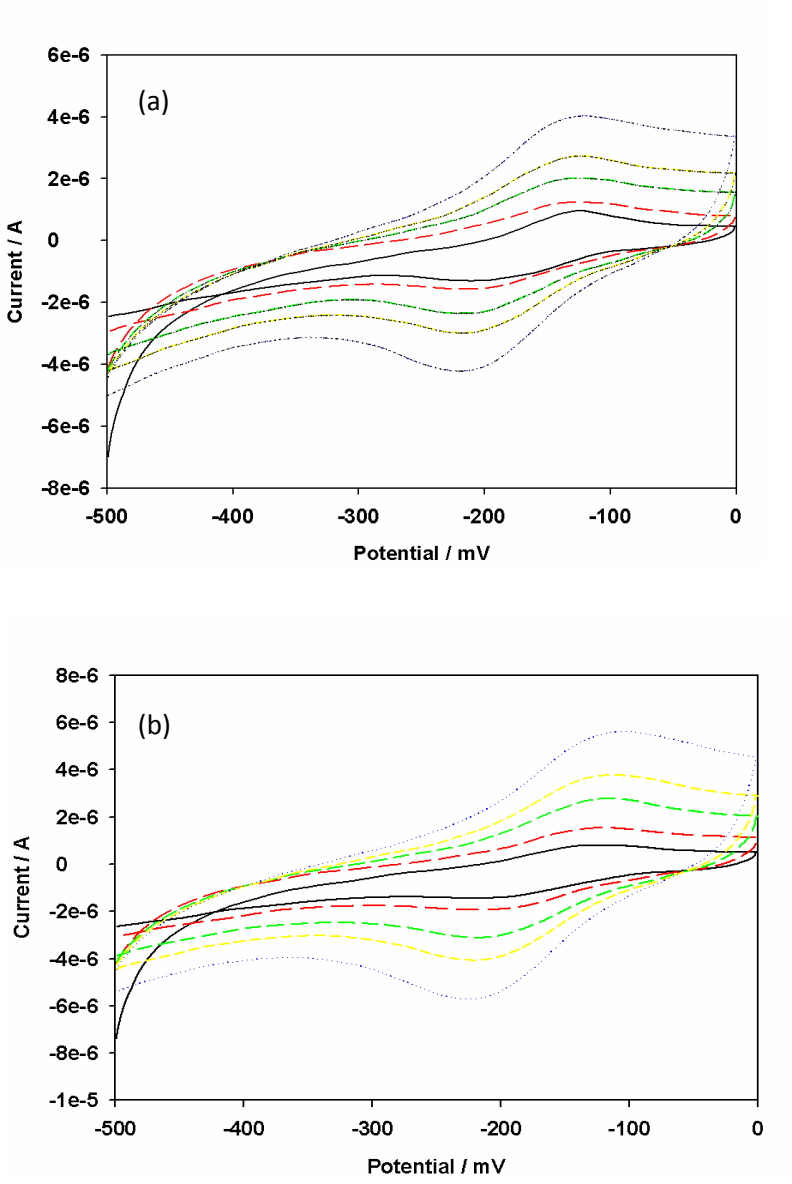

3.3 Electrochemical characteristics of the electrode

The stepwise assembly of the immunosensor was monitored cyclic-voltammetrically in acetate buffer pH 6.5 and the results are shown in Figure 5. The CV of the bare GCE is shown as Figure 5a. The bare GCE did not exhibit any redox chemistry over the potential window (-500 to 0 mV) used in the study. The GCE|PTH gave a quasi reversible electrochemistry with a peak separation of ~62 mV at 10 mV/s (Figure 5b). The redox couple can be ascribed to the electrochemistry of the PTH film on the GCE. The peak currents increased after the modification of GCE|PTH with AuNP (Figure 5e). The reason for this increase is that nanometer-sized particles of colloidal gold behave like a conducting wire or electron conducting tunnel, which makes it easier for the electron transfer to take place. However, the peak currents decreased (Figure 5d) after AFB_1-BSA conjugate was incorporated to

produce GCE|PTH|AuNP|AFB_1-BSA-conjugate, which indicated that the relatively insulating AFB_1-BSA conjugate was immobilized on the electrode surface. The subsequent blocking of possible active sites with HRP to form GCE|PTH|AuNP|AFB_1-BSA-conjugate|HRP immunosensor system decreased the CV peak current due to the adsorption of the protein, HRP (Figure 5c). Surface concentration (Γ^*) values of 7.06 x 10^{-11} and 9.65 x 10^{-10} mol/cm^2 were calculated for GCE|PTH and GCE|PTH|AuNP|AFB_1-BSA-conjugate electrode systems, respectively.

Figure 5. CV's of **(a)** bare GCE; **(b)** GCE|PTH|; **(c)** GCE|AuNP|PTH|AFB_1-BSA-conjugate|HRP-blocked; **(d)** GCE|AuNP|PTH|AFB_1-BSA-conjugate and **(e)** GCE|AuNP|PTH. Conditions: acetate buffer ph 6.5; scan rate = 10 mV/s.

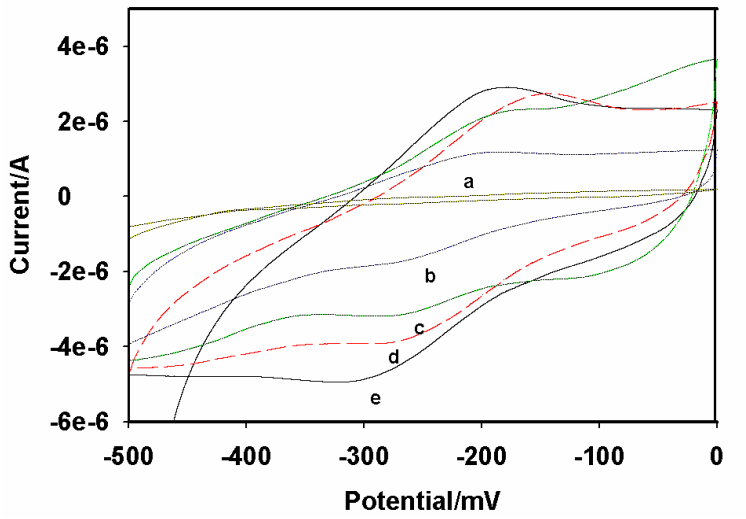

3.4 Assay of the HRP enzymatic catalytic activity

Horseradish peroxidase was used in the preparation of the immunosensors to block possible uncovered active sites on the GCE|AuNP|PTH|AFB_1-BSA-conjugate in order to avoid non-specific adsorption. Experiments were performed with hydrogen peroxide to ascertain if HRP was indeed immobilized on the electrode. Figure 6 depicts the CV's of the proposed immunosensor in the presence and absence of H_2O_2. A redox couple representing the electrochemistry of PTH was observed in the absence of H_2O_2 (Figure 6a). However, an enhancement of the cathodic peak and a concomitant decrease of the anodic peak current were observed in the presence of 3.2 µM H_2O_2 (Figure 6b). It can thus be concluded that HRP was attached to the immunosensor surface and it retained its enzymatic catalytic activity [21], which is coupled to the PTH electron transfer process shown below.

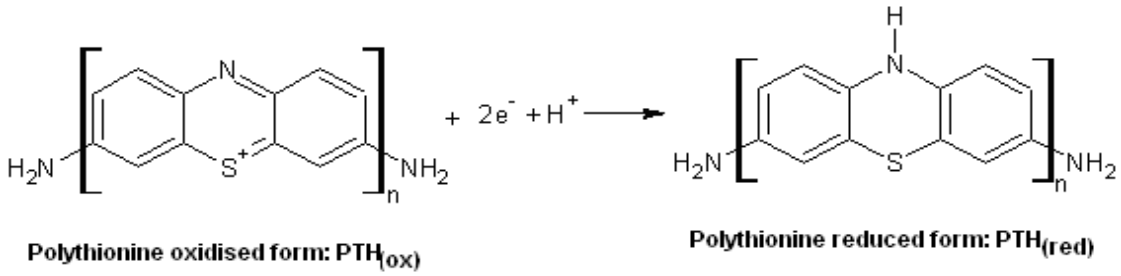

The optimal amount of H_2O_2 required for the immunosensing reaction with GCE|AuNP|PTH|AFB_1-BSA-conjugate|HRP-blocked electrode system was determined from steady-state amperometry experiments performed at -175 mV. As shown in Figure 7, the sensor gave a maximum response at 3.2 µM H_2O_2. At H_2O_2 concentrations higher than 3.2 µM, the sensor response decreased owing to the irreversible transition of the immobilized HRP to its inactive form [32]. As a result, 3.2 µM H_2O_2 was chosen for the immunosensing experiments.

Figure 6. CV's of AFB_1 immunosensor (GCE|AuNP|PTH|AFB_1-BSA-conjugate|HRP-blocked) in acetate buffer (pH 6.5): in the absence (a), and presence (b), of 3.2 µM H_2O_2. Scan rate = 10 mV/s.

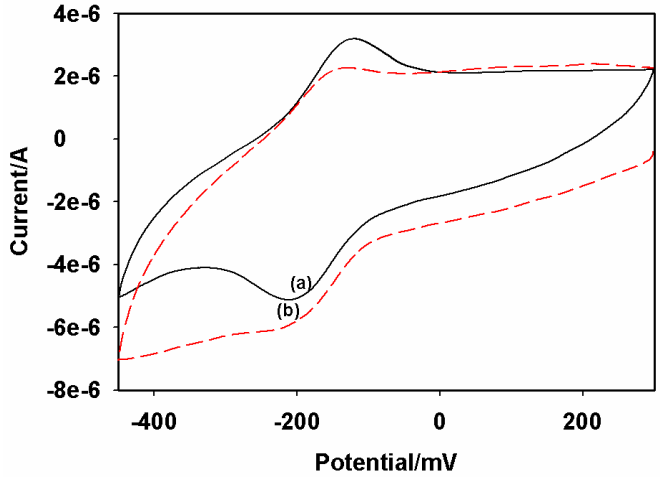

Figure 7. Steady-state amperometric responses of AFB_1 immunosensor (GCE|AuNP|PTH|AFB_1-BSA-conjugate|HRP-blocked) to H_2O_2 in acetate buffer (pH 6.5) at -175 mV. Inset: H_2O_2 calibration curve obtained from the steady state responses.

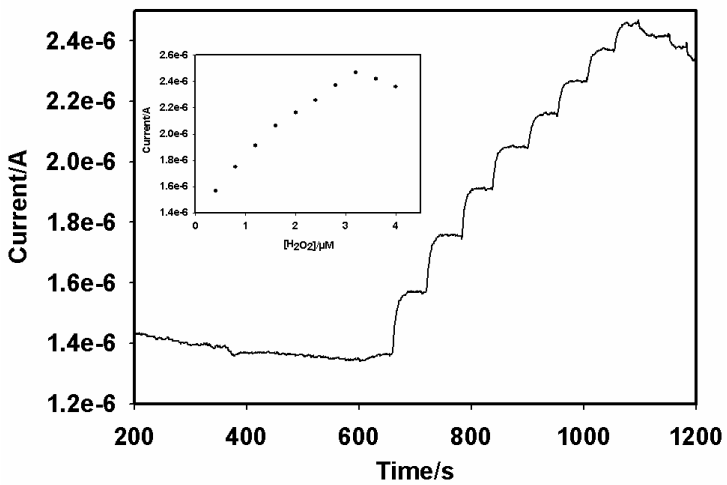

The effect of pH on the immunosensor was studied for pH's 4.5 to 6.5 at 25 °C. In order to retain the bioactivity of both AFB_1-BSA conjugate and HRP, pH 6.5 was chosen as the optimal pH. Although 37 °C is the best incubation temperature for antibody-antigen reactions, immunoproteins and HRP do not maintain their activities for a long time at this temperature. As a result 25 °C was used in all experiments.

3.4 Performance of the immunosensor

The responses of the immunosensor to AFB_1 were recorded with DPV as shown in Figure 8 for 0 – 3 ng/mL AFB_1. As expected, the peak current was inversely proportional to the analyte concentration. The detection principle is based on the inhibition of the active centre of HRP by the formation of antigen-antibody complex. The observed current is attributed to the catalytic response of the adsorbed HRP to H_2O_2. The formation of the antigen-antibody complex introduces a local current change at the sites of the adsorbed HRP due to the inhibition of the H_2O_2 reduction reaction. The attenuation of the DPV response is dependent on AFB_1 concentration as shown in Figure 8 and it is attributable to the increase in electron transfer resistance of adsorbed HRP [33] caused by the insulating properties of the complex formed by the binding of AFB_1-BSA conjugate and anti-AFB_1 antibody.

Figure 8. DPV responses of AFB_1 immunosensor (GCE|AuNP|PTH|AFB_1-BSA-conjugate|HRP-blocked), for 0 - 3 ng/mL AFB_1 (mixed with anti-AFB_1 antibody) in acetate buffer (pH 6.5) containing 3.2 μM of H_2O_2. DPV experimental conditions: scan rate = 20 mV/s; pulse amplitude = 10 mV; and pulse width = 50 ms.

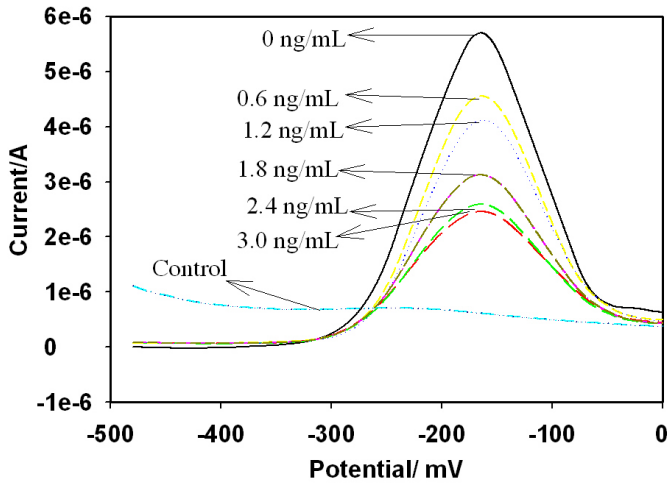

Figure 9. Calibration plot of AFB_1 immunosensor. Conditions are as given in Figure 8.

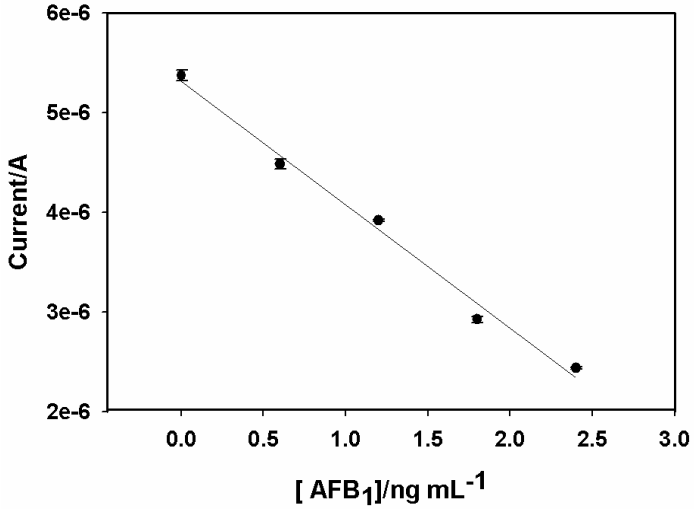

The calibration graph of the AFB_1 immunosensor (Figure 9) plotted from DPV results gave DLR, sensitivity and LOD values of 0.6 - 2.4 ng/mL, 1.23 x 10^{-6} A/(ng/mL) and 0.07 ng/mL, respectively. The DPV measurements were carried out in triplicates. The relative standard deviations of the DPV responses were 3.1%, 2.9%, 2.4% and 5.1% for 0.6, 1.2, 1.8 and 2.4 ng/mL, respectively, indicating acceptable level of precision.

Table 1. Comparison of the analytical parameters of AFB_1 immunosensor.

Immunosensor	**DLR (ng/mL)**	**LOD (ng/mL)**	**Reference**
96-well screen printed microplate	0.05 – 2	0.03	[15]
Pt|PSSA|PANi|Anti-AFB_1	0.1 - 0.6	0.1	[18]
GCE|Nafion|RTIL|TiO_2|AuNP|Anti-AFB_1-HRP	0.1 – 12	0.05	[20]
GCE|AuNP|PTH|AFB_1-BSA-conjugate|HRP-blocked	0.6 - 2.4	0.07	This work

4. Conclusions

The DLR and LOD of the immunosensor were compared with those of other electrochemical AFB_1 immunosensors [15, 18, 20] as shown in Table 1. The values of these sensor parameters for the PTH-based immunosensor are in good agreement with those reported by other laboratories. In addition, the sensor exhibited high sensitivity and good reproducibility. These characteristics of the immunosensor show that it can be used to screen food products for AFB_1, since the DLR and LOD values cover the FAO's limit of 2 ppb AFB_1 in food samples [5]. The immunosensing procedure reported in this study eliminated the requirement of secondary labeled antibodies as is the case in conventional electrochemical immunosensors based on ELISA techniques.

Acknowledgements

This study was funded by the National Research Foundation (NRF) of South Africa.

References

1. Cole, R.J.; Cox, R.H. *Handbook of Toxic fungal metabolites*. Academic Press: New York, 1981.
2. International Agency for Research on Cancer. *IARC Monographs on the evaluations of Carcinogenic Risks to Humans*. IARC: Lyon, 1993; vol. *56*, pp. 489-521.
3. Moss, O.M. Risk assessment for aflatoxins in foodstuffs. *Int. Biodeterior. Biodegrad*. **2002,** *50*, 137-142.
4. Miraglia, M.; Brera, C.; Colatosti, M. Application of Biomarkers to Assessment of Risk to Human Health from Exposure to Mycotoxins. *Michrochem. J*. **1996,** *54*, 472-477.
5. Van Egmond, H.P.; Jonker, A.R.O. *Worldwide regulations for mycotoxins in food and feed in 2003*. FAO Food and Nutrition paper 81: Report of the Food and Agriculture Organization of the United Nations: Rome, 2004.

6. Fernandez, A.; Belio, R.; Ramos, J. J.; Sanz, M.C.; Saez, T. Aflatoxins and their metabolites in the tissues, faeces and urine from lambs feeding on an aflatoxin-contaminated diet. *J. Sci. Food Agric*. **1997**, *74*, 161-168.
7. Jaimez, J.; Fente, C.A.; Vazquez, B.I.; Franco, C.M.; Capeda, A.; Mahhuzier, G.; Prognon, P. Application of the assay of aflatoxins by liquid chromatography with fluorescence detection in food analysis. *J. Chromatog. A*. **2000,** *882*, 1-10
8. Stroka, J.; Anklam, E. New strategies for the screening and determination of aflatoxins and the detection of aflatoxin-producing moulds in food and feed. *Trends. Anal. Chem.* **2002**, *21*, 90-95.
9. Dutta, T.K.; Das, P. Isolation of aflatoxigenic strains of *Aspergillus* and detection of aflatoxin B_1 from feeds in India. *Mycopathologia* **2000,** *151*, 29-33.
10. Kolosova, A.Y.; Shim, W.B.; Yang, Z.Y.; Eremin, S.A.; Chung, D. H. Direct competitive ELISA based on a monoclonal antibody for detection of aflatoxin B1. Stabilization of ELISA kit components and application to grain samples. *Anal. Bioanal. Chem*. **2006,** *384*, 286-294.
11. Ayciek, H.; Aksoy, A.; Saygi, S. Determination of aflatoxin levels in some dairy and food products consumed in Ankara, Turkey. *Food Control*. **2005,** *16*, 263-266.
12. Zheng, H.; Humphney, C. W.; King, R.S.; Richard, J.L. A review of rapid methods for the analysis of aflatoxins. *Mycopathologia.* **2005**, *159*, 1-9.
13. Yaroglu, T.; Oruc, H.H.; Tayar, M. Aflatoxin M_1 levels in cheese samples from some provinces of Turkey. *Food Control*. **2005**, *16*, 883-885.
14. Rastogi, S.; Divedi, P.D.; Khanna, S.K.; Das, M. Detection of Aflatoxin M_1 contamination in milk and infant milk products from Indian markets by ELISA. *Food Control*. **2004**, *15*, 287-290.
15. Piermarini, S.; Micheli, L.; Ammida, N.H.S.; Palleschi, G.; Moscone, D. Electrochemical immunosensor array using a 96-well screen-printed microplate for aflatoxin B_1 detection. *Biosens. Bioelectron.* **2007,** *22*, 1434-1440.
16. Micheli, L.; Grecco, R.; Badea, M.; Moscone, D.; Palleschi, G. An electrochemical immunosensor for aflatoxin M_1 determination in milk using screen-printed electrodes. *Biosens. Bioelectron*. **2005,** *21*, 588-596.
17. Pemberton, R.M.; Pittson, R.; Biddle, N.; Drago, G.A.; Hart, J.P. Studies towards the development of a screen-printed carbon electrochemical immunosensor array for mycotoxins: A sensor for Aflatoxin B_1. *Anal. Lett.* **2006,** *39*, 1573-1586.
18. Owino, J. H. O.; Ignaszak, A.; Al-Ahmed, A.; Baker, P.G. L.; Alemu, H.; Ngila, J.C.; Iwuoha, E. I. Modelling of the impedimetric responses of an aflatoxin B_1 immunosensor prepared on an electrosynthetic polyaniline platform. *Anal. Bioanal. Chem*. **2007,** *388*, 1069-1074.
19. Adanyi, N.; Levkovets, I. A.; Rodriguez-Gil, S.; Ronald, A.; Varadi, M.; Szendro, I. Development of immunosensor based on OWLS technique for determining Aflatoxin B1 and Ochratoxin A. *Biosens. Bioelectron.* **2007,** *22,* 797-802.
20. Sun, A.; Qi, Q.; Dong, Z. L.; Liang, K.Z. An electrochemical enzyme immunoassay for aflatoxin B1 based on bio-electrocatalytic reaction with room-temperature ionic liquid and nanoparticle-modified electrodes. *Sens. & Instrumen. Food Qual.* **2008**, *2*, 43-50.
21. Ruan, C.; Yang, F.; Lei, C.H.; Deng, J.Q. Thionine covalently tethered to multilayer horseradish peroxidise in a self assembled monolayer as an electron transfer mediator. *Anal. Chem.* **1998**, *70*, 1721-1725.

22. Xiao, Y.; Ju, H.; Chen, H.Y. A reagentles hydrogen peroxide sensor based on incorporation of horseradish peroxidise in poly(thionine) film on a monolayer modified electrode., *Anal.Chim Acta.* **1999,** *391*, 299-306.
23. Reid, G.D.; Whittaker, D.J.; Day, M.A.; Creely, C.M.; Tuite, E.M.; Kelly, Beddard, G.S. Ultrafast Electron-Transfer Reactions between Thionine and Guanosine Bases. *J. Am.Chem. Soc.* **2001**, *123*, 6953-6954.
24. Dohno, C, Stemp, E.D.A.; Barton, J. K. Fast Back Electron Transfer Prevents Guanine Damage by Photoexcited Thionine Bound to DNA. *J. Am.Chem. Soc.* **2003**, *125*, 9586-9587.
25. Storhoff, J.J.; Elghanian, R.; Music, R.C.; Markin, C.A.; Lestinger, R.L. One pot colorimetric differentiation of polynucleotides with single base imperfections using gold nanoparticles. *J. Am.Chem. Soc.* **1998**, *120*, 1959-1964.
26. Tang, D.P.; Yuan, R.; Chai, Y.Q.; Dai, J.Y.; Zhong, X.; Liu, Y. A novel immunosensor based on immobilization of hepatitis B surface antibody on platinum electroe modified colloidal gold and polyvinyl butyral as matrices via electrochemical impedance spectroscopy. *Bioelectrochem.* **2004***, 65*, 15-22.
27. Xu, S.Y.; Han, X.Z. A novel method to contruct a third generation biosensor: self assembling gold nanoparticles on thiol-functionalized poly (styrene-co-acrylic acid) nanospheres. *Biosens. Bioelectron*. **2004,** *19*, 1117-1120.
28. Liu, S.Q.; Leech, D.; Ju, H.X. Application of colloidal gold in protein immobilization, electron transfer and biosensing. *Anal. Lett.* **2003**, *36*, 1-17.
29. Yuan, R.; Tang, D.; Chai, Y.; Zhong, X.; Liu, Y.; Dai. Ultrasensitive potentiometric immunosensor based on SA and OCA techniques for immobilization of HBsAb with colloidal Au and Polyvinyl Butyral as matrixes. *Langmuir.* **2004**, *20*, 7240-7245.
30. Yang, R.; Ruan, C.; Dai, W.; Deng, J.; Kong, J. Electropolymerization of thionine in neutral aqueous media and H_2O_2 biosensor based on poly(thionine). *Electrochim. Acta.* **1999**, *44*, 1585-1596.
31. Murray, R.W. In: Bard, A.J. (ed), Electroanalytical chemistry. Marcel Dekker: New York, 1984; vol. *13*, p.191.
32. Ju, H.X.; Yan, G.F.; Chen, H.Y. Enzyme-Linked Immunoassay of α-1-Fetoprotein in Serum by Differential Pulse Voltammetry. *Electroanalysis.* **1999**, *11*, 124-129.
33. Lu, X; Bai, H; He, P; Cha, Y; Yang, G; Tan, L; Yang, Y.A reagentless amperometric immunosensor for α-1-fetoprotein based on gold nanowires and ZnO nanorods modified electrode. *Anal.Chim.Acta.* **2008**, *615*, 158-164.